# Ho3+-doped Y3NbO7 transparent ceramic elaborated by air pre-sintering and post-HIP treatment as potential LASER gain material at 2 $\mu$m

Louis Cornet, Simon Guené-Girard, Jean-Marc Heintz, Rémy Boulesteix, Alexandre Maître, Veronique Jubera

▶ **To cite this version:**

Louis Cornet, Simon Guené-Girard, Jean-Marc Heintz, Rémy Boulesteix, Alexandre Maître, et al.. Ho3+-doped Y3NbO7 transparent ceramic elaborated by air pre-sintering and post-HIP treatment as potential LASER gain material at 2 $\mu$m. Optical Materials, 2023, 144, pp.114319. 10.1016/j.optmat.2023.114319 . hal-04197983

**HAL Id: hal-04197983**
**https://hal.science/hal-04197983v1**

Submitted on 6 Sep 2023

**HAL** is a multi-disciplinary open access archive for the deposit and dissemination of scientific research documents, whether they are published or not. The documents may come from teaching and research institutions in France or abroad, or from public or private research centers.

L'archive ouverte pluridisciplinaire **HAL**, est destinée au dépôt et à la diffusion de documents scientifiques de niveau recherche, publiés ou non, émanant des établissements d'enseignement et de recherche français ou étrangers, des laboratoires publics ou privés.

# $Ho^{3+}$-doped $Y_3NbO_7$ transparent ceramic elaborated by air pre-sintering and post-HIP treatment as potential LASER gain material at 2 microns

L. Cornet[1], S. Guene-Girard[1], J-M Heintz[1], R. Boulesteix[2], A. Maître[2], V. Jubera[1*]

1- Univ. Bordeaux, CNRS, Bordeaux INP, ICMCB, UMR 5026, F-33600 Pessac, France

2- Institute for Research on Ceramics (IRCER), UMR CNRS 7315, Univ. Limoges, F-87068 Limoges, France

* Corresponding author: veronique.jubera@u-bordeaux.fr

**Abstract**

In the framework of the development of new laser materials at the lowest limit of the mid-IR range, the cubic $Y_3NbO_7$ matrix has been doped by trivalent holmium. Fine powders were prepared through a liquid phase synthesis and highly densified using a two-stage sintering process: i) natural sintering was performed in air to reach relative density higher than 95 %; ii) Hot Isostatic Pressure was applied to obtain fully dense and, consequently, transparent ceramics. The resulting microstructures were examined and then related to sintering parameters such as temperature and pressure. Refractive index, transmission and luminescence properties were measured and presented for the first time on a bulk material. These encouraging results showed that the $Ho^{3+}$-doped $Y_3NbO_7$ compound is a promising potential candidate as a new laser material.

**Key words**: holmium, niobate, transparent ceramic, luminescence

## 1-Introduction

The $RE_3NbO_7$ (RE = rare earth elements) niobate family presents versatile crystal structures depending on the RE cationic radius [1]–[6]. They are studied for their magnetic [7]–[12], ionic conductivity [13], [14], thermal properties [15] as well as for their luminescent properties [16], [17]. Among them, the yttrium phase presents high interests as a potential candidate for laser properties. The substitution of yttrium by holmium on its site, coupled with the existence of a local disorder caused by oxygen vacancies, induces a large spectral emission from the visible range to the mid infrared [18]–[20]. This large spectral distribution can be a great advantage regarding the absorption or laser range tuning capability in a LASER configuration. The high stability of the yttrium cubic host lattice at high temperature could lead to fully dense and transparent ceramics after sintering. First results concerning a non-doped phase have been recently reported by Huang *et al.* [21], after An *et al.* [22]. These authors mentioned the manufacturing of niobate transparent ceramics whose chemical compositions crystallize in a similar way to the $Lu_3NbO_7$ phase.

However, the preparation of transparent ceramics, especially in the niobate family, is not trivial. The main limitation concerns light scattering due to residual porosity. Different methods promote the elimination of porosity in ceramics, such as using pressure-assisted sintering techniques. Among them, Hot Isostatic Pressing (HIP) is usually used to obtain highly transparent ceramics of different materials such as $MgAl_2O_4$ [23], YAG [24]–[26], $Y_2O_3$ [27], $Al_2O_3$ [28] or $Lu_2O_3$ [29]. This technique consists of performing sintering in an inert atmosphere at a given temperature under high pressure of 200 to 400 MPa. Compared to usual Hot Pressing (HP) or Spark Plasma Sintering (SPS), HIP allows not only decreasing the sintering temperature due to the applied pressure but also limiting carbon contamination due to glass-encapsulation technique for instance [30]. This ensures high optical quality for a wide variety of transparent ceramics. Transparent ceramics of niobate have been already obtained by SPS [22]. Nevertheless, due to the high ionic conductivity of this phase, ionic mobility can be activated by the applied electric field during SPS, leading to untimely decomposition of the desired phase [31]. To our knowledge, HIP was never reported for the preparation of doped-$Y_3NbO_7$ transparent ceramics.

In this study, we propose to investigate the shaping and the optical properties of $Ho^{3+}$ doped $Y_3NbO_7$ compound. The HIP sintering parameters have been studied in order to reach a high density of this doped compound, which is a primordial criterion for obtaining maximum transmission rates. The microstructure of sintered bodies were analyzed as a function of the sintering temperature and pressure. Optical properties such as refractive index, transmission, absorption, emission and decay times are reported for the first time.

## 2- Materials and methods

### *2.1 Particle syntheses and shaping*

$Ho^{3+}$-doped $Y_3NbO_7$ powders were prepared by a co-precipitation method using $NbCl_5$ (99.9% purity, Aldrich), $HoCl_3.6H_2O$ (99.99% purity, Merck), and $YCl_3.6H_2O$ (99.99% purity, Alfa Aesar) as reactants for the synthesis. The experimental procedure is described elsewhere [32]. The holmium content in the holmium chlorine powder was evaluated by chemical analysis (ICP/OES). A 0.6% molar content of holmium was selected on the basis of a previous investigation which indicated that this concentration is a good compromise between emission intensity and energy transfer

The powders were ball-milled for 2 hours (400 rpm), sieved and dry-pressed by Cold Isostatic Pressing (CIP) at 150 MPa into a green body. The obtained pellets were heat–treated at 1600°C during 2, 4 or 6 hours in air to obtain dense samples (> 95 % $d_{th}$) without residual open porosities. An example of microstructure is illustrated in supplementary information **Figure SI1**. Then, Hot Isostatic Pressing (HIP)

was performed on each pellet during 1 hour at 1600°C, 1650°C or 1700°C in a pressure of 190 MPa [31]. After HIP, a re-oxidation step was applied during 2 hours at 1100°C in flowing oxygen ($O_2$).

The sintered pellets were polished on both sides using $Al_2O_3$ (30 μm, 10 μm) and $CeO_2$ (2 μm) particles dispersed in water. The final thickness of the pellets ranged between 0.7 and 1 mm.

*2.2 Scanning electron microscopy (SEM)*

Scanning electron microscopy (SEM) analysis was performed using a TESCAN Vega II SBH SEM to characterize the main microstructural features (grain size and morphology, and porosity) of the densified ceramics. Average grain size was determined by the intercept method [33] by counting the number of grains traversed by straight lines of known length. In order to obtain a satisfying statistical result, the method was applied to at least three micrographs per sample. The grain size is taken as the intercept length (no corrective factor).

*2.3 Transmission analyses*

Transmission spectra were obtained using an Agilent Cary 5000 equipment operating in the UV to IR range.

*2.4 Refractive index*

The determination of the experimental refractive index of the best optical quality pellet was performed by ellipsometry in the visible range on a JA Wollam-2000 (acquisition range: 200 to 1700 nm) and on a J.A. Wollam IR-VASE Mark II (acquisition range from 1700 nm to 8000 nm).

*2.5 Luminescence spectroscopy and decay time measurements*

The emission spectra were obtained using a Horiba Jobin Yvon HR 640 monochromator equipped with a PbSe detectors. A 455 nm laser diode was used as the excitation source. All the measurements were performed at room temperature. The luminescence spectra were corrected for the sensitivity of the detectors and response of grating (600 lines).

Lifetime measurements were realized in the desired range with a 10 nm step-by for each wavelength using as a pumping source an Optical Parametric Oscillator (OPO) centered at 525 or 980 nm. Bandpass filters were used in order to eliminate the second harmonics. Infrared lifetime measurements were carried out using an Edinburgh FLS1000 spectrometer coupled with a digital Tektronix oscilloscope to record the time-dependent decay. During the measurements, all the samples were carefully placed in the same position to ensure good comparability between the spectra. All the measurements mentioned above were made at room temperature.

**3- Results and discussion**

Optical micrographs of the nine sintered pellets are presented on Figure 1. All these ceramics present a transparent aspect. Some of them broke during the re-oxidation process suggesting the presence of internal stress and/or microstructural heterogeneities.

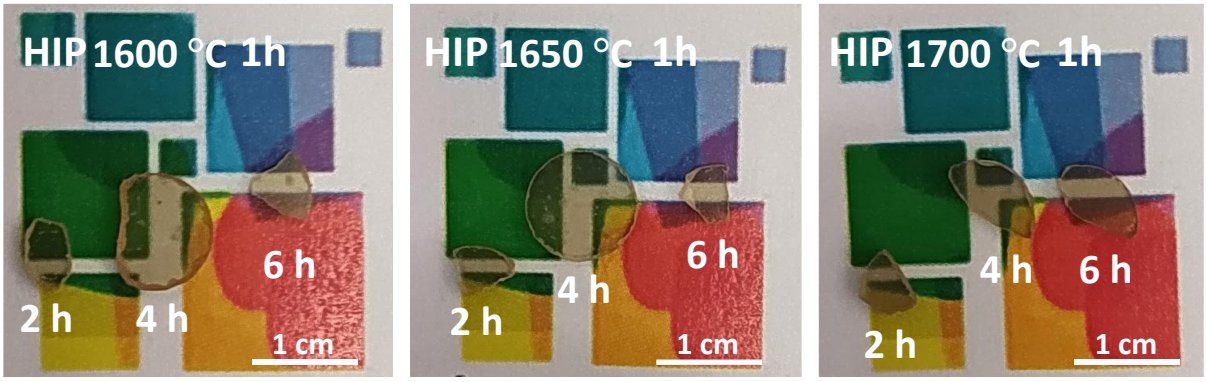


**Figure 1-** Optical micrographs of $Y_3NbO_7:Ho^{3+}$ transparent ceramics after HIP and reoxidation as a function of sintering conditions. The temperature of the 1 hour HIP treatment is indicated on the top of the picture. 2h, 4h and 6h indicate the dwell times of the natural sintering step at 1600°C, applied after shaping by CIP.

As mentioned previously, the relative density of the heat-treated pellets reaches 95%. Unfortunately, due to the small size of the pellets, broken after HIP, and the large uncertainty associated with the measurement of their volume, the experimental densities of the final HIPed bodies are not given here. However, the corresponding microstructures, observed by SEM, are illustrated in **Figure 2**. All samples appear almost fully dense with little inter- or intragranular residual porosity. Whatever the duration of the first sintering treatment at 1600°C, all pellets HIP-treated at 1600°C (Fig. 2 (a-c)) present similar aspects. A significant grain growth is observed as the HIP temperature increases, regardless of the pre-sintering protocol. For the 1600°C HIP heat-treatment, the grain size is about 3 µm. It increases up to an average value of 5-6 µm and finally 9-10 µm for 1650°C and 1700°C, respectively. The diameter of pores remains less than 1 µm and small with respect to the grain size. These first results demonstrate that two-stage sintering including a pre-sintering step in air and a post-densification step by HIP, appears as a very efficient way to fully densify this niobate material at limited temperature *(i.e.* 1600°C) and isostatic pressure (*i.e.* 190 MPa). A better control of the HIP parameters should make possible the complete removal of the intergranular porosity and should avoid the occurrence of intragranular porosity.

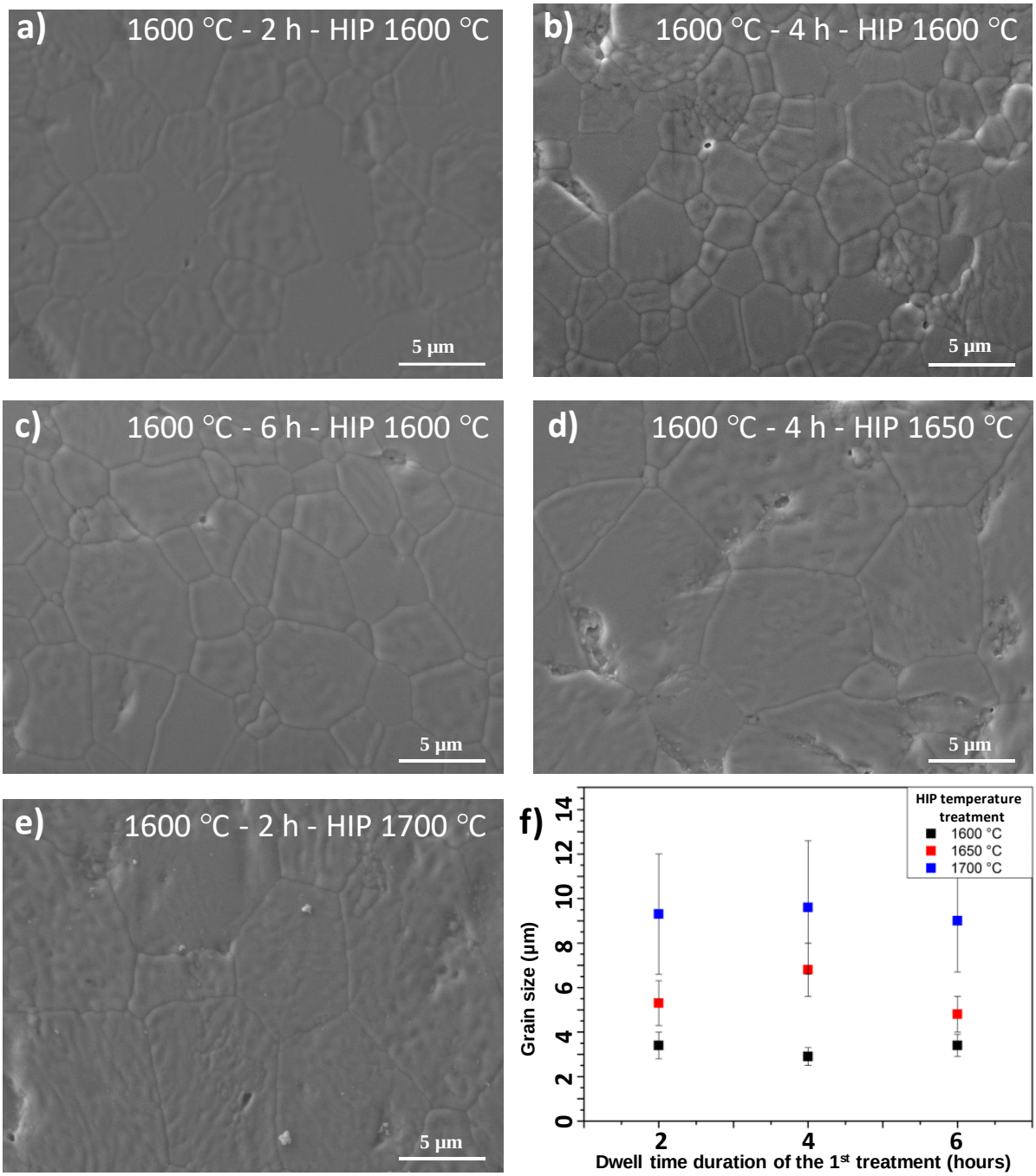


**Figure 2-** (a-e) SEM micrographs of polished and thermally revealed surfaces of $Y_3NbO_7:Ho^{3+}$ ceramics and (f) evolution of the grain size as a function of the sintering conditions (temperature and time of pressureless sintering and post-HIP temperature with a dwell time of 1 h).

The transmission spectra are given in **Figure 3**, together with the theoretical maximum transmission values due to specular reflection of the material, calculated with equation (1).

$$T_{max}(\lambda) = \frac{2n(\lambda)}{[n(\lambda)^2+1]} \qquad (1)$$

The refractive index, *n(λ)*, was determined using experimental ellipsometry measurements (described in supplementary information **Figure SI2**). A value of 1.99 ± 0.01 at around 2 µm was obtained, in good agreement with the values reported by Huang *et al.* [21]. The $Ho^{3+}$-doped compound presents a large optical window between 310 nm and 8 µm. This corresponds to the bandgap mainly due to the niobium oxygen charge transfer (value close to the one reported in the literature [34]) and the IR absorption edge, respectively. The absorption lines detected from the visible to infrared range confirms the doping of the $Y_3NbO_7$ compound by $Ho^{3+}$ cations.

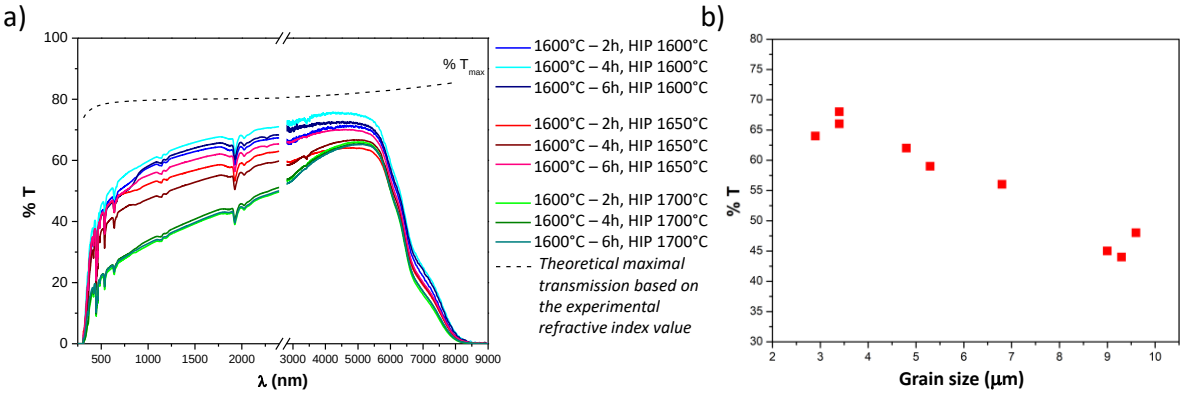


**Figure 3-** (a) Transmission spectra of $Y_3NbO_7$:$Ho^{3+}$ transparent ceramics according to sintering conditions (HIP dwell time was 1 h); (b) evolution of the maximum transmission levels at 2 µm as a function of grain size.

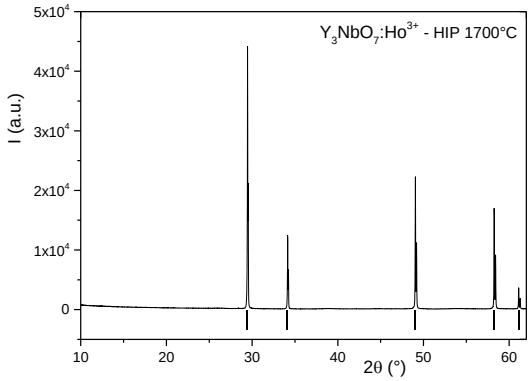


**Figure 4-** X-Ray diffraction pattern of the (1600°C-6hours, HIP 1700°C) pellet for which the lowest transmission is observed. This pattern confirms the absence of phase decomposition as all the peaks are attributed to the $Y_3NbO_7$ compound (indexation with the 00-036-1353 JCPDS file).

Post-HIP sintering temperature seems to have more influence on the transmission values than the pressureless sintering duration itself, meaning that this first pre-sintering step is not so crucial. The best transmission levels correspond to the pellets HIPed at 1600°C, which was the lowest HIP sintering temperature. Among these samples, the pellet treated 4 hours has the highest transmission value, equal to about 69 % at a wavelength of 2 µm. The increase of the temperature of the HIP treatment up to 1700°C is strongly detrimental to the optical properties, as the maximum transmission at 2 µm drops to 48 % for the 4 hours pre-treated pellet. As we have discarded by X-Ray Diffraction the presence of a secondary phase (**Figure 4**), this loss in transmission could be a consequence of several parameters. First, an increase of the grain size is observed, since an increase of the HIP temperature results in a grain growth (**Figure 3**). The second reason relies on the change in size and distribution of the residual porosity (*i.e.* coalescence of pores), accelerated by the increase of the HIP temperature. Third, a higher reduction of the pellets is expected for the longest duration for HIP treatments. But a similar post-re-oxidation step was applied on all of them. This may stabilize $Nb^{4+}$ cations as absorbing centers. Finally, as a primary result and using such a sintering process, an average grain size of 3.5 µm yielding maximum transmission seems suitable for a mid-IR application.

In complement, microluminescence mappings were conducted in the visible range to detect potential segregation of the doping element at the grain boundaries. To avoid surface artefacts, the intensity was recorded below the surface at different depths. A good homogeneity of the spectral distribution and intensity was observed in a probed surface of about 40 µm² (**Figure SI3**), which tends to confirm a lack of $Ho^{3+}$ ions segregation within the pellets at a 1 µm² scale.

Photoluminescence spectroscopy was performed on the pellets post-sintered by HIP at temperatures ranging between 1600°C and 1700°C, under excitation in the $^5G_6$,$^5F_1$ levels at 450 nm (**Figure 5 (a)**). The global luminescence intensity in the 1800-2200 nm range is promoted by the increase of the crystallites size, the maximum being reached for the samples HIPed at 1650°C and 1700°C for which the intensity is nearly equivalent. The effective bandwidth of the $^5I_7 \rightarrow {}^5I_8$ transition was calculated according to the following equation (2) [35]:

$$\Delta\lambda_{eff} = \int_{1800}^{2200} \frac{I(\lambda)}{I_{max}}\, d\lambda \qquad (2)$$

where $I(\lambda)$ is the value of the emission intensity and $I_{max}$, the maximum of the emission intensity. A value of 172 nm is obtained whatever the pellet, which is twice the value calculated for $Ho^{3+}$-doped YAG [36]. This enlargement of the emission peaks in this niobate host lattice is a direct consequence of the more disordered crystalline structure and coordination polyhedra of the holmium cations compared to YAG for example, as discussed in references [18]–[20].

The decay curve of the $^5I_7$-$^5I_8$ transition (**Figure 5 (b)**) was performed on the most transparent pellet (pre-sintered 4 h at 1600°C/HIP 1 h at 1600°C). It has been fitted with a single exponential law and a τ value equal to 8.09 ms is obtained. This value is comparable to the experimental one reported for $Ho^{3+}$-doped YAG laser materials containing a similar $Ho^{3+}$ ions volume density [37].

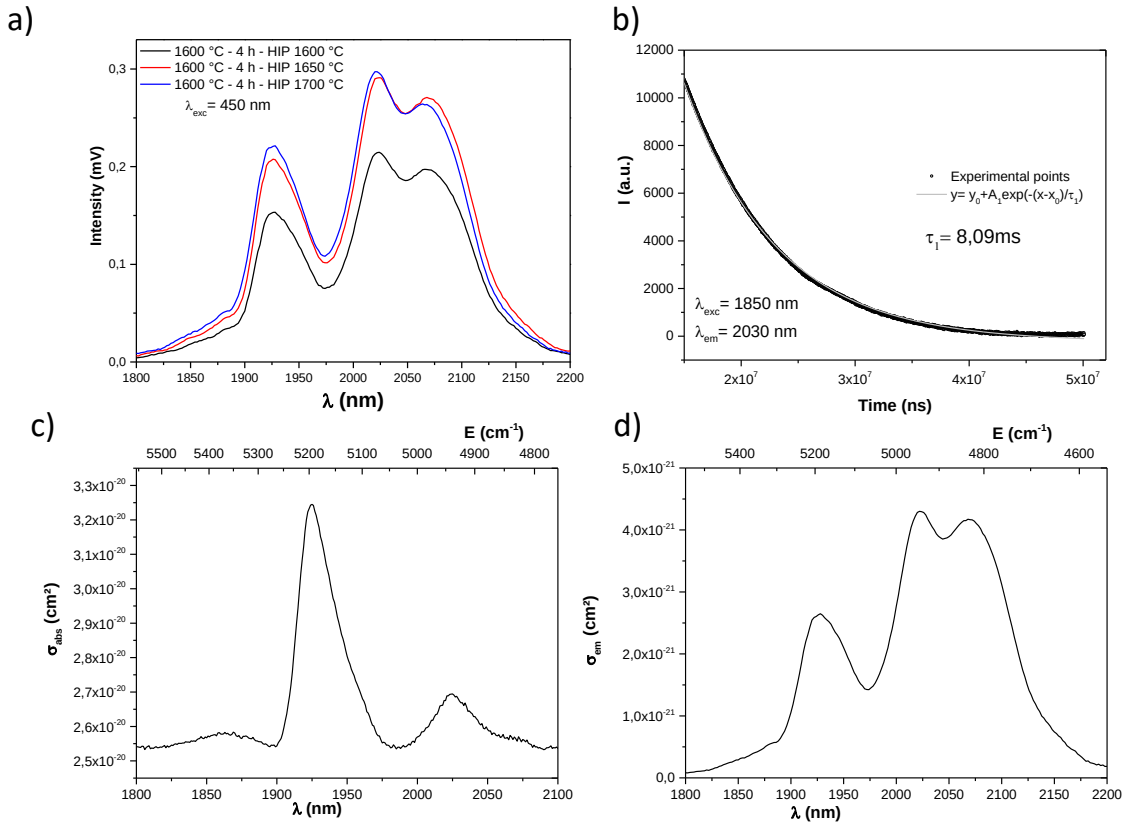


**Figure 5-** (a) Luminescent characterizations of $Y_3NbO_7$:$Ho^{3+}$ emission as function of the HIP temperature (same pre-sintering at 1600°C-4 h). (b) Decay curve of the maximal emission. (c) Estimated absorption cross section and (d) calculated emission cross section of the sample. These last characterizations were performed on the sample pre-sintered 4 h at 1600°C.

A first absorption cross section estimation in the wavelength range 1800-2100 nm is proposed in Figure 4 (c). To avoid the contribution of light scattering linked to the presence of residual porosity, the baseline of the experimental transmission curve has been shifted to fit to the expected maximum value at a given wavelength (estimation based on the refractive index value). The absorption cross section was calculated using equation (3).

$$\sigma_{abs}(\lambda) = \frac{OD\ln(10)}{Nl} \qquad (3)$$

where *OD* is the Optical Density calculated from the transmission curve, $OD = -log_{10}\left(\frac{I}{I_0}\right)$ with $I$, the incident beam and $I_0$ the transmitted one; $N$ (ions.cm$^{-3}$) the number of $Ho^{3+}$ ions per cm$^3$ and $l$ (cm) the pellet thickness. A maximum is observed at a wavelength of 1925 nm (E = 5200 cm$^{-1}$).

A first calculation of the spontaneous radiative lifetime $\tau_{rad}$ is proposed in **Figure SI4**. But as the value obtained is not satisfying due to the low quality of the experimental transmission graph, we have decided to propose a possibly underestimated emission cross section, based on the experimental decay time value (Figure 4 (d)), according to equation (4).

$$\sigma_{em}(\lambda) = \frac{\lambda^4}{8\pi n^2 c\tau}\frac{I(\lambda)}{\int_{1800}^{2200} I(\lambda)d\lambda} \qquad (4)$$

with *I(λ)* (a.u.) emission intensity at $\lambda$; n the experimental refractive index; *c* (3.10$^8$ m.s$^{-1}$); $\tau$ (s) was taken as the experimental lifetime and not the $\tau_{rad}$ value. At this first stage, we expect a value of the emission cross section much higher than 4.10$^{-21}$cm² in the laser range at around 2.1 µm which is about 26 % of an equivalent $Ho^{3+}$-doped YAG crystal.

These first spectroscopic characterizations tend to confirm that the $Ho^{3+}$-doped compound presents interesting spectral characteristics. First, a large absorption range makes possible the use of several excitation wavelengths. Second, for LASER applications, a wide emission range could also be associated to a wider laser tuning capability than other materials. But the optical quality of ceramics has to be improved to generate a gain effect.

**Conclusion**

Optical $Ho^{3+}$-doped $Y_3NbO_7$ transparent ceramics have been obtained. A two-stage sintering process coupling both pressureless sintering and HIP, appears as a promising method to fully densify this compound. However, intragranular residual porosity is detrimental to a good transmission value. So the preparation process including post-treatment has still to be improved. This will help to avoid light scattering or potential stabilization of absorbing centers which may result from point defects such as $Nb^{4+}$ cations. The spectroscopic characteristics of the densified $Ho^{3+}$-doped $Y_3NbO_7$ are investigated for the first time. The wide emission band at 2 micrometers and its corresponding decay time appear to be competitive with the $Ho^{3+}$-doped YAG compounds which is one of the most investigated material for LASER applications in the Mid-IR range.

**Acknowledgement**

The authors thank the CNRS. This study was carried out with financial support of the Nouvelle Region d'Aquitaine (MISTRAL program n°2017-1R50311 and HICEMIR program n◦ 2020-RNA20435), in the frame of "the Investments for the future" Program IdEx Bordeaux – LAPHIA (ANR-10-IDEX-03-02), Program Labex Sigma-LIM Limoges (ANR-10-LABX-0074-01) and the French Research National Agency (ANR program HEMERALD ANR-20-CE08-0016-01). We also acknowledge the support from the LIGHT S&T Graduate Program (PIA3 Investment for the Future Program, ANR-17-EURE-0027).

The authors thanks B. Giroire, T. Girardeau and F. Paumier from Institute PPRIME-CNRS for the determination of the refractive index, L. Viers and M. Vandenhende from IRCEr for their help in the HIP process, V-A. Garcia Rivera, Y. Messadecq from Centre d'Optique, Photonique et Laser (COPL) and F. Calzavara (ICMCB) for the dedicated time in the decay time measurements. This last point was performed in the frame of the International Associated Laboratory IRP LuMAQ CNRS.

## References

[1] H. P. Rooksby and E. A. D. White, « Rare-Earth Niobates and Tantalates of Defect Fluorite- and Weberite-Type Structures », *J. Am. Ceram. Soc.*, vol. 47, n° 2, p. 94-96, févr. 1964, doi: 10.1111/j.1151-2916.1964.tb15663.x.

[2] L. Cai and J. C. Nino, « Complex ceramic structures. I. Weberites », *Acta Crystallogr. B*, vol. 65, n° 3, p. 269-290, juin 2009, doi: 10.1107/S0108768109011355.

[3] H. J. Rossell, « Fluorite-related phases Ln3MO7, Ln = rare earth, Y or Sc, M = Nb, Sb, or Ta », *J. Solid State Chem.*, vol. 27, n° 1, p. 115-122, janv. 1979, doi: 10.1016/0022-4596(79)90150-6.

[4] Y. Yamasaki and Y. Sugitani, « Flux Growth of Double Oxides of Niobium and Rare-earth Elements ($Ln_3NbO_7$ ) », *Bull. Chem. Soc. Jpn.*, vol. 51, n° 10, p. 3077-3078, oct. 1978, doi: 10.1246/bcsj.51.3077.

[5] M. Ptak, B. Pilarek, A. Watras, P. Godlewska, I. Szczygieł, and J. Hanuza, « Structural, vibrational and optical properties of $Eu^{3+}$-doped $Gd_3NbO_7$ niobates – The mechanism of their structural phase transition », *J. Alloys Compd.*, vol. 810, p. 151892, nov. 2019, doi: 10.1016/j.jallcom.2019.151892.

[6] S. Lopatin, L.N. Avervyanova, and I. Belyaev, Effect of ion radii and the atom electronegativity on the type of crystal-structure of $A_2B_2O_7$ combination compounds, Zh. Neorg. Khim. 30 (1985) 867e872.

[7] A. N. Klimenko, Yu. S. Kozlov, V. S. Sergeev, and E. A. Pastukhov, « High temperature phase transitions in rare-earth element niobates $R_3NbO_7$ », *Thermochim. Acta*, vol. 209, p. 331-338, nov. 1992, doi: 10.1016/0040-6031(92)80211-E.

[8] J. F. Vente, R. B. Helmholdt, and D. J. W. IJdo, « The Structure and Magnetic Properties of $Pr_3MO_7$ with M = Nb, Ta, and Sb », *J. Solid State Chem.*, vol. 108, n° 1, p. 18-23, janv. 1994, doi: 10.1006/jssc.1994.1003.

[9] A. Kahn-Harari, L. Mazerolles, D. Michel, and F. Robert, « Structural Description of $La_3NbO_7$ », *J. Solid State Chem.*, vol. 116, n° 1, p. 103-106, avr. 1995, doi: 10.1006/jssc.1995.1189.

[10] L. Cai and J. C. Nino, « Structure and dielectric properties of $Ln_3NbO_7$ (Ln=Nd, Gd, Dy, Er, Yb and Y) », *J. Eur. Ceram. Soc.*, vol. 27, n° 13-15, p. 3971-3976, janv. 2007, doi: 10.1016/j.jeurceramsoc.2007.02.077.

[11] Y. Doi, Y. Harada, and Y. Hinatsu, « Crystal structures and magnetic properties of fluorite-related oxides $Ln_3NbO_7$ (Ln=lanthanides) », *J. Solid State Chem.*, vol. 182, n° 4, p. 709-715, avr. 2009, doi: 10.1016/j.jssc.2008.12.012.

[12] M. Inabayashi, Y. Doi, M. Wakeshima, and Y. Hinatsu, « Synthesis, crystal structures and magnetic properties of fluorite-related compounds $Ce_3MO_7$ ( M = Nb, Ta) », *J. Solid State Chem.*, vol. 254, p. 150-154, oct. 2017, doi: 10.1016/j.jssc.2017.07.022.

[13] J.-H. Lee, M. Yashima, M. Kakihana, and M. Yoshimura, « Phase Diagram and Oxygen-Ion Conductivity in the $Y_2O_3$-$Nb_2O_5$ System », *J. Am. Ceram. Soc.*, vol. 81, n° 4, p. 894-900, janv. 2005, doi: 10.1111/j.1151-2916.1998.tb02424.x.

[14] A. Chesnaud, M.-D. Braida, S. Estradé, F. Peiró, A. Tarancón, A. Morata, and G. Dezanneau, « High-temperature anion and proton conduction in $RE_3NbO_7$ (RE = La, Gd, Y, Yb, Lu) compounds », *J. Eur. Ceram. Soc.*, vol. 35, n° 11, p. 3051-3061, oct. 2015, doi: 10.1016/j.jeurceramsoc.2015.04.014.

[15] L. Chen, P. Wu, P. Song, and J. Feng, « Potential thermal barrier coating materials: $RE_3NbO_7$ ( RE =La, Nd, Sm, Eu, Gd, Dy) ceramics », *J. Am. Ceram. Soc.*, vol. 101, n° 10, p. 4503-4508, oct. 2018, doi: 10.1111/jace.15798.

[16] Lj Đačanin Far, A. Ćirić, Z. Ristić, J. Periša, T. Dramićanin, S.R. Lukić-Petrović, and M.D. Dramićanin, « Photoluminescence of $Y_3NbO_7:Eu^{3+}$ powders », *Ceram. Int.*, p. S0272884222021332, juin 2022, doi: 10.1016/j.ceramint.2022.06.130.

[17] A. Walasek, E. Zych, J. Zhang, and S. Wang, « Synthesis, morphology and spectroscopy of cubic $Y_3NbO_7$:Er », *J. Lumin.*, vol. 127, n° 2, p. 523-530, déc. 2007, doi: 10.1016/j.jlumin.2007.02.063.

[18] K.-Y. Kim, U-C. Chung, B. Mutulet, F. Weill, A. Demourgues, J. Rossit, J-M. Heintz, A. Veillere and V. Jubera, « Tailoring the Composition of $Eu^{3+}$-Doped $Y_3NbO_7$ Niobate: Structural Features and Luminescent Properties Induced by Spark Plasma Sintering », *Inorg. Chem.*, vol. 56, n° 8, p. 4495-4503, avr. 2017, doi: 10.1021/acs.inorgchem.7b00088.

[19] K.-Y. Kim, A. Durand, J.-M. Heintz, A. Veillere, and V. Jubera, « Spectral evolution of $Eu^{3+}$ doped $Y_3NbO_7$ niobate induced by temperature », *J. Solid State Chem.*, vol. 235, p. 169-174, mars 2016, doi: 10.1016/j.jssc.2015.12.023.

[20] S. Guene-Girard, J. Courtois, M. Dussauze, J-M. Heintz, A. Fargues, J. Roger, M. Nalin, T. Cardinal, and V. Jubera, « Comparison of structural and spectroscopic properties of $Ho^{3+}$-doped niobate compounds », *Mater. Res. Bull.*, vol. 143, p. 111451, nov. 2021, doi: 10.1016/j.materresbull.2021.111451.

[21] M. Huang, L. Li, Y. Feng, X. Zhao, W. Pan, and C. Wan, « $Y_3NbO_7$ transparent ceramic series for high refractive index optical lenses », *J. Am. Ceram. Soc.*, vol. 104, n° 11, p. 5776-5783, nov. 2021, doi: 10.1111/jace.17953.

[22] L. An, A. Ito, and T. Goto, « Fabrication of transparent $Lu_3NbO_7$ by spark plasma sintering », *Mater. Lett.*, vol. 65, n° 19-20, p. 3167-3169, oct. 2011, doi: 10.1016/j.matlet.2011.07.010.

[23] K. Tsukuma, « Transparent $MgAl_2O_4$ Spinel Ceramics Produced by HIP Post-Sintering », *J. Ceram. Soc. Jpn.*, vol. 114, n° 1334, p. 802-806, 2006, doi: 10.2109/jcersj.114.802.

[24] L. Chrétien, L. Bonnet, R. Boulesteix, A. Maître, C. Sallé, and A. Brenier, « Influence of hot isostatic pressing on sintering trajectory and optical properties of transparent Nd:YAG ceramics », *J. Eur. Ceram. Soc.*, vol. 36, n° 8, p. 2035-2042, juill. 2016, doi: 10.1016/j.jeurceramsoc.2016.02.021.

[25] A. Ikesue and K. Kamata, « Microstructure and Optical Properties of Hot Isostatically Pressed Nd:YAG Ceramics », *J. Am. Ceram. Soc.*, vol. 79, n° 7, p. 1927-1933, juill. 1996, doi: 10.1111/j.1151-2916.1996.tb08015.x.

[26] S.-H. Lee, E. R. Kupp, A. J. Stevenson, J. M. Anderson, G. L. Messing, X. Li, E. C. Dickey, J. Q. Dumm, V. K. Simonaitis-Castillo, and G. J. Quarles, « Hot Isostatic Pressing of Transparent Nd:YAG Ceramics », *J. Am. Ceram. Soc.*, vol. 92, n° 7, p. 1456-1463, juill. 2009, doi: 10.1111/j.1551-2916.2009.03029.x.

[27] A. Ikesue and K. Kamata, « Fabrication of Transparent Ce:$Y_2O_3$ Ceramics Using a HIP », *J. Ceram. Soc. Jpn.*, vol. 103, n° 1203, p. 1155-1159, 1995, doi: 10.2109/jcersj.103.1155.

[28] A. Krell, P. Blank, H. Ma, T. Hutzler, and M. Nebelung, « Processing of High-Density Submicrometer $Al_2O_3$ for New Applications », *J. Am. Ceram. Soc.*, vol. 86, n° 4, p. 546-53, avr. 2003, doi: 10.1111/j.1151-2916.2003.tb03339.x.

[29] Z. M. Seeley, J. D. Kuntz, N. J. Cherepy, and S. A. Payne, « Transparent $Lu_2O_3$:Eu ceramics by sinter and HIP optimization », *Opt. Mater.*, vol. 33, n° 11, p. 1721-1726, sept. 2011, doi: 10.1016/j.optmat.2011.05.031.

[30] J. Mouzon, A. Maître, L. Frisk, N. Lehto, M. Odén, "Fabrication of transparent yttria by HIP and the glass-encapsulation method", *J. Eur. Ceram. Soc.*, vol. 29 n°2, p. 311-316, 2009, https://doi.org/10.1016/j.jeurceramsoc.2008.03.022.

[31] S. Guené-Girard *et al.*, « Développement de céramiques transparentes de type niobates dopées aux terres rares: vers de nouvelles sources LASER infrarouges », Université de Bordeaux, (France), 2021, http://www.theses.fr/2021BORD0031/document.

[32] S. Guené-Girard, V. Jubera, L. Viers, R. Boulesteix, A. Maître, and J.-M. Heintz, « Liquid phase synthesis and sintering of $Y_3NbO_7$ », *Ceram. Int.*, vol. 46, n° 16, p. 26361-26367, nov. 2020, doi: 10.1016/j.ceramint.2020.02.190.

[33] H. Abrams, « Grain size measurement by the intercept method », *Metallography*, vol. 4, n° 1, p. 59-78, févr. 1971, doi: 10.1016/0026-0800(71)90005-X.

[34] R. Abe, M. Higashi, Z. Zou, K. Sayama, Y. Abe, and H. Arakawa, « Photocatalytic Water Splitting into $H_2$ and $O_2$ over $R_3TaO_7$ and $R_3NbO_7$ (R = Y, Yb, Gd, La): Effect of Crystal Structure on Photocatalytic Activity », *J. Phys. Chem. B*, vol. 108, n° 3, p. 811-814, janv. 2004, doi: 10.1021/jp036300v.

[35] M. Hongisto, A. Veber, N. G. Boetti, S. Danto, V. Jubera, and L. Petit, « Transparent $Yb^{3+}$ doped phosphate glass-ceramics », *Ceram. Int.*, vol. 46, n° 16, p. 26317-26325, nov. 2020, doi: 10.1016/j.ceramint.2020.01.121.

[36] L. Viers, « Approche des mécanismes de frittage non conventionnel et des propriétés spectroscopiques de céramiques transparentes dopées holmium pour des lasers émettant dans le moyen infrarouge », Université de Limoges (France), 2021, https://theses.hal.science/tel-03202768.

[37] J. Šulc, M. Nemec, D. Vyhlidal, H. Jelínková, K. Nejezchleb, and J. Polák, « Holmium doping concentration influence on Ho:YAG crystal spectroscopic properties », in *Solid State Lasers XXX: Technology and Devices*, W. A. Clarkson et R. K. Shori, Éd., Online Only, United States: SPIE, mars 2021, p. 34. doi: 10.1117/12.2578284.

## Supplementary informations

### SI1- Example of microstructure before HIP treatment

The $Ho^{3+}$-doped $Y_3NbO_7$ heat –treated at 1600°C during 4h is illustrated below. The lack of intragrain porosity and the small size grain are targeted before the HIP treatment.

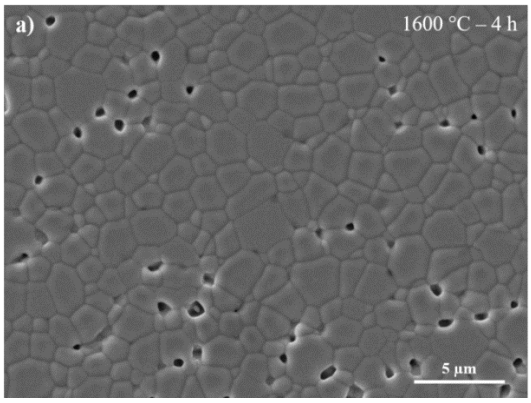


**Figure SI1**- $Ho^{3+}$-doped $Y_3NbO_7$ heat –treated at 1600°C during 4h microstructure

## SI2- Refractive index n and attenuation coefficient k measurements of $Y_3NO_7:Ho^{3+}$ transparent ceramic

An ellipsommetry measurement consists of using polarized radiation at different angles of incidence on the surface of a sample.

Ellipsommetry measures the quantity ρ: $\rho = tan\varphi e^{i\Delta}$

with $\Delta$,the difference in phase between the incident and reflected radiation and ψ the decrease in field strength.

A polarized wave can be described by projection on the orthogonal planes p and s as the addition two orthogonal plane waves such as:$\widetilde{E_x} + \widetilde{E_y} = \widetilde{E_{xo}} e^{i\delta x} + \widetilde{E_y} e^{i\delta y}$ with x along the p plane and y along the s plane. Jones' matrix is used to describe the change in polarization of a wave when it interacts with matter:

$$\begin{bmatrix} E_x \\ E_y \end{bmatrix}_r = \begin{bmatrix} j_{xx} & j_{xy} \\ j_{yx} & j_{yy} \end{bmatrix} \begin{bmatrix} E_x \\ E_y \end{bmatrix}_i$$

In the case of an isotropic material, ellipsometry measures the ratio of two complex numbers $\frac{\widetilde{r_p}}{\widetilde{r_s}}$
(Fresnel coefficients) matrix :

$$\begin{bmatrix} E_p \\ E_s \end{bmatrix}_r = \widetilde{r_s} \begin{bmatrix} \frac{\widetilde{r_p}}{\widetilde{r_s}} & 0 \\ 0 & 1 \end{bmatrix} \begin{bmatrix} E_{xi} \\ E_{yi} \end{bmatrix} i$$

Thus, the corresponding ellipsometry equation is given by :
$\rho = tan\varphi e^{i\Delta} = \frac{\widetilde{r_p}}{\widetilde{r_s}} = \frac{r_p}{r_s} e^{i(\delta_p - \delta_s)}$ and $tan\varphi = \frac{r_p}{r_s}$ and $\Delta = \delta_p - \delta_s$

The Fresnel equation alloy the calculation of the complex refractive index value of the materials :

$\tilde{r_s} = \frac{\widetilde{n_i} cos\theta_i - \widetilde{n_t} cos\theta_t}{\widetilde{n_i} cos\theta_i + \widetilde{n_t} cos\theta_t}$ and $\tilde{r_p} = \frac{\widetilde{n_t} cos\theta_i - \widetilde{n_i} cos\theta_t}{\widetilde{n_t} cos\theta_i + \widetilde{n_i} cos\theta_t}$

The analysis of the experimental data uses the theoretical model of the general oscillator which makes it possible to take into account the presence of optical absorbers in the wavelength domain considered.
The refinement is done by regression on the values of $\Delta$ and ψ. The model response is generated and compared to the measurement until a minimum square mean error is obtained. The dielectric function of the material ($\varepsilon_1$; $\varepsilon_2$) then the index ( $\tilde{n} = ik = \sqrt{\varepsilon_1 - i\varepsilon_2}$ ) are extracted from this model.
The method determines the refractive index value over the entire measurement range (300 nm to 8 µm).
Finally, for $Eu^{3+}$ ion-doped ceramics, we obtain a refractive index of 2.01 +/-0.01 at 2 µm and 1.99 +/-0.01 at 2 µm for $Ho^{3+}$ ion-doped ceramics.
Note that these data are conditioned by the quality of the ceramic and the quality of the polishing.

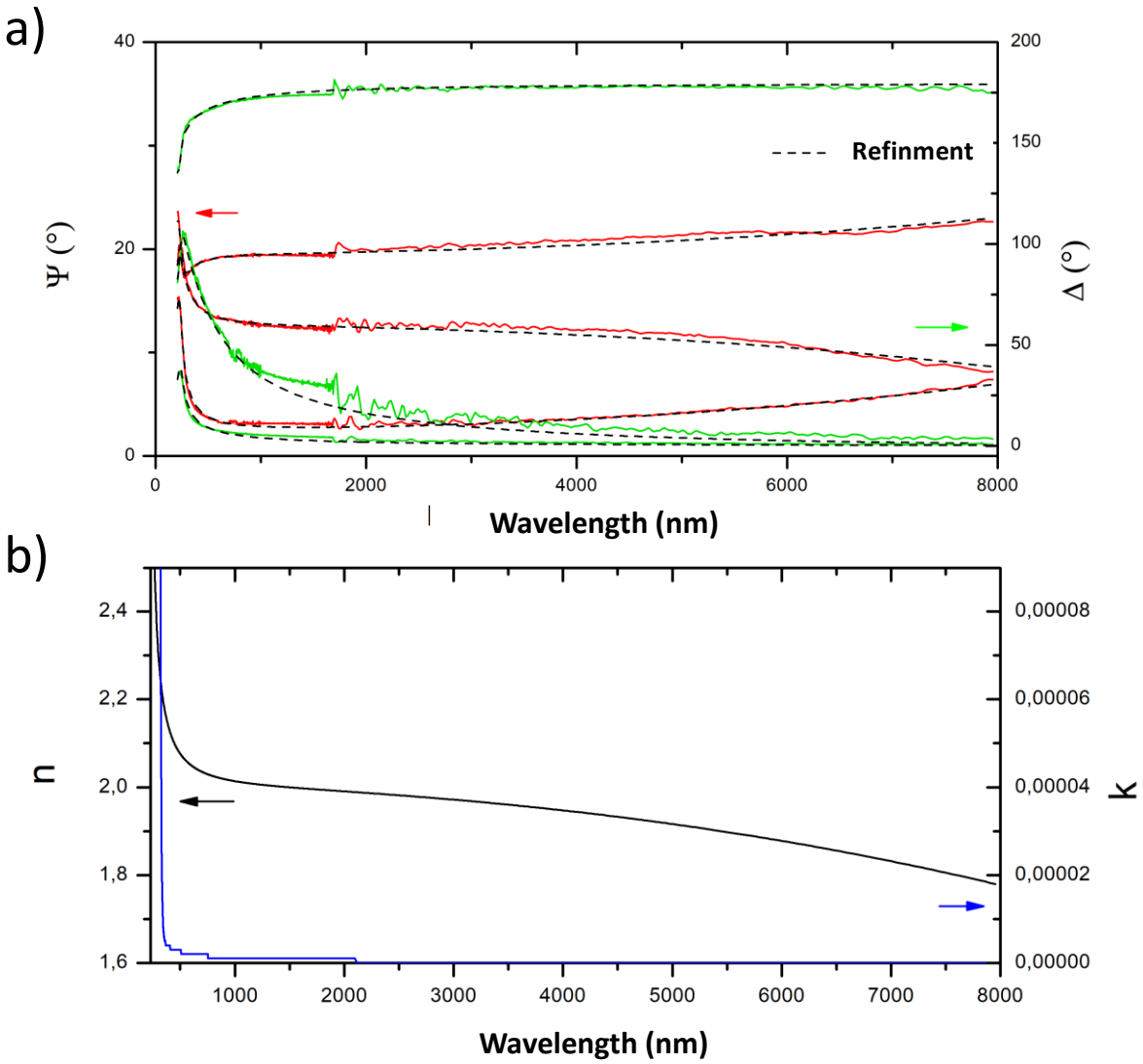


**Figure SI2-** n refractive index dispersion and k attenuation coefficient of $Y_3NbO_7$: $Ho^{3+}$ ceramics.

## SI3- Microluminescence characterization of $Y_3NbO_7:Ho^{3+}$ transparent ceramic

Microluminescence mapping was obtained with a LabRAM 800-HR spectrophotometer (Horiba Jobin-Yvon) equipped with an Olympus microscope objective. A stabilized 450 nm laser diode beam was injected to excite the $Ho^{3+}$ ions and collect the visible luminescence. These data are reported in supplementary information

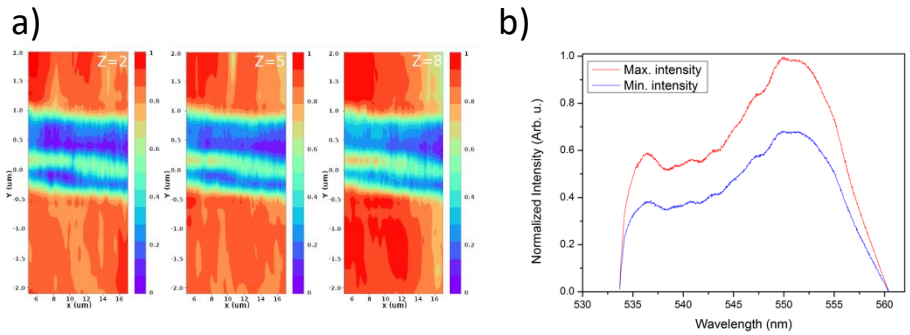


**Figure SI3**- Microluminescence mapping obtained under a 450 nm excitation and corresponding to the integrated $^5F_4,^5S_2 \rightarrow ^5I_8$ visible transition: a) 3D mapping of $Y_3NbO_7:Ho^{3+}$ with different z values (3 depths), b) Spectral distribution obtained in the lowest and highest intensity area (blue and red curves respectively) of the $Y_3NbO_7:Ho^{3+}$ pellet.

An area revealing a polishing defect is selected to enhance the intensity modulation resulting from the surface relief **(Figure SI2a**). The emission spectra are illustrated in the highest and lowest intensity area as an indicator of the global amplitude of the mapping scale. No modification of the spectral distribution was observed and a difference of about 68% is obtained between both (**Figure SI2b)**. The mapping was then normalized between 0 (intensity in the scratch) and 1, maximum intensity outside this defected zone. Consequently, the scratch (central blue zone) is clearly visible as the $Ho^{3+}$ intensity drops drastically. As the mapping is performed from z= 2 to z= 8, the $Ho^{3+}$ intensity tends to be more and more constant with a really light contrast color outside the scratch, for the deepest acquisition at z=8. This is in agreement with the reduction of the surface topology effect on the collected intensity and tends to confirm a lack of segregation of the doping element within the grains. But being the spatial resolution equal to 1µm², the grain boundaries cannot be discriminated.

## SI4- Attempt to calculate the spontaneous radiative lifetime $\tau_{rad}$

The spontaneous radiative lifetime $\tau_{rad}$ corresponds to a radiative decay time considering that spontaneous emission is the only mechanism for depopulating the excited state. It was deduced from the estimated absorption cross section as following:

$$\frac{1}{\tau_{rad}} = \frac{G_f}{G_i}\frac{8\pi c n^2}{\overline{\lambda^4}}\int_{1800}^{2100}\sigma_{abs}(\lambda)d\lambda$$

where $G_f$ and $G_i$ are the multiplicity of the $^5I_7$ and $^5I_8$ levels, equal to 17 and 15, respectively; c, the light velocity ($3.10^8$ m.s$^{-1}$); $\overline{\lambda}$ the wavelength at which half the integrated emission area is reached ($\overline{\lambda}$ = 2026 nm). The estimated $\tau_{rad}$ is about 0.5 ms but it seems to be far too short considering the order of magnitude reported for other $Ho^{3+}$ doped compounds such as YAG [1]. In addition, being the experimental decay time of the niobate close to that of $Ho^{3+}$-YAG, one can imagine that the de-excitation processes between both materials are similar and so there is no reasonable explanation for such a discrepancy (nearly one order of magnitude) except the high uncertainty introduced by the calculated absorption cross section.

[1] L. Viers, « Approche des mécanismes de frittage non conventionnel et des propriétés spectroscopiques de céramiques transparentes dopées holmium pour des lasers émettant dans le moyen infrarouge », 2021, https://theses.hal.science/tel-03202768.